HHS Public Access

Author manuscript

Curr Eye Res. Author manuscript; available in PMC 2015 June 02.

Published in final edited form as:

Curr Eye Res. 2015 April ; 40(4): 368–377. doi:10.3109/02713683.2014.924147.

Nicotine Accelerates Diabetes-Induced Retinal Changes

Adam Boretsky[1,2], **Praveena Gupta**[3], **Nima Tirgan**[3], **Rong Liu**[3,6], **Bernard F. Godley**[3], **Wenbo Zhang**[3], **Ronald G. Tilton**[3,4,5], and **Massoud Motamedi**[1,3]

[1] Center for Biomedical Engineering, The University of Texas Medical Branch, Galveston, TX 77555, USA

[2] Human Pathophysiology and Translational Medicine, The University of Texas Medical Branch, Galveston, TX 77555, USA

[3] Department of Ophthalmology and Visual Sciences, The University of Texas Medical Branch, Galveston, TX 77555, USA

[4] Department of Internal Medicine, Division of Endocrinology, The University of Texas Medical Branch, Galveston, TX 77555, USA

[5] Stark Diabetes Center, The University of Texas Medical Branch, Galveston, TX 77555, USA

[6]Department of Ophthalmology, Tongji Hospital, Tongji Medical College, Huazhong University of Science and Technology, Wuhan, China

Abstract

Purpose: To investigate the effects of nicotine on retinal alterations in early stage diabetes in an established rodent model.

Materials and Methods: Sprague-Dawley rats were examined using a combination of confocal scanning laser ophthalmoscopy and spectral domain optical coherence tomography to determine changes in retinal structure in response to nicotine exposure, diabetes and the combined effects of nicotine and diabetes. Diabetes was induced by a single injection of 65 mg/kg streptozotocin and nicotine injections were administered subcutaneously daily. Retinal thickness in the superior, inferior, nasal and temporal quadrants were determined based on SD-OCT volume scans (20° × 20°) centered on the optic disc. Segmentation of discrete retinal layers was performed on a subset of SD-OCT cross-sections to further examine changes in each treatment group. Survival of neurons within the ganglion cell layer (GCL) was assessed by confocal morphometric imaging.

Results: The control group did not experience any significant change throughout the study. The nicotine treatment group experienced an average decrease in total retinal thickness (TRT) of 9.4 μm with the majority of the loss localized within the outer nuclear layer (ONL) as determined by segmentation analysis ($P < 0.05$). The diabetic group exhibited a trend toward decreased TRT while segmentation analysis of the DR group revealed significant thinning within the ONL ($P <$

Correspondence should be addressed to: Massoud Motamedi, Ph.D. University of Texas Medical Branch Center for Biomedical Engineering 301 University Blvd. Galveston, TX 77555-0625 Phone: 409/772-8363 Fax: 409/772-0751 mmotamed@utmb.edu.

Declaration of Interests

The authors report no conflicts of interest.

0.05). The combination of nicotine and diabetes revealed a significant increase of 8.9 μm in the TRT ($P < 0.05$) accompanied by a decrease in the number of GCL neurons.

Conclusions: We demonstrated significant temporal changes in retinal morphology in response to nicotine exposure, diabetes and with the combined effects of nicotine and diabetes. These findings may have implications in determining treatment strategies for diabetic patients using products containing nicotine such as cigarettes, smokeless tobacco, electronic cigarettes, or smoking cessation products.

Keywords

SD-OCT; SLO; diabetes; nicotine; retinal thickness; neurons

Introduction

Diabetic retinopathy (DR) is a prominent global health issue that poses a substantial threat to visual function. Despite available treatments, DR remains the leading cause of blindness amongst working age adults(1). The hallmark of DR is vascular pathology that includes microaneurysms, macular edema and neovascularization(2, 3). However, numerous clinical and experimental studies of DR have reported evidence of early-stage visual dysfunction and neuronal cell loss (4-20) which precedes alterations in retinal vasculature that are commonly used as a diagnostic metric.

Smoking has a profound impact on overall ocular health(21). Deleterious effects of smoking have been shown to enhance the development and progression of numerous ocular diseases, including age-related macular degeneration (22-24), glaucoma (25, 26), cataracts (27, 28) and DR (29-31). At the early stages of type 1 diabetes, cigarette smoking and genetic susceptibility to hypertension are important risk factors for microvascular complications(32). It has been shown that smoking leads to a higher incidence of retinopathy (33) and accelerated progression of retinopathy (34) in patients with type 1 diabetes.

Nicotine is one of the major toxic components found in cigarettes, electronic cigarettes, smokeless tobacco and smoking cessation products. Recently, nicotine has been shown to stimulate angiogenesis (35, 36), alter retinal pigment epithelial (RPE) cell morphology and function (37), and significantly decrease electroretinogram (ERG) responses (38-40). The impact of nicotine on experimentally induced diabetes has never been explored with respect to temporal alterations in retinal morphology and edema *in vivo*. Spectral domain optical coherence tomography (SD-OCT) is commonly used clinically to observe morphological changes in the retina and this technique has also been used to investigate numerous experimental models of injury and disease(41, 42). Multiple studies have demonstrated a strong correlation between retinal thickness measurements using SD-OCT data and histology in rodents(43, 44). In this study, we used non-invasive multimodal imaging and morphologic analysis to quantitate changes in the retinal ultrastructure and neurons within the ganglion cell layer (GCL) of an inducible type 1 diabetic rat model under the influence of systemic nicotine exposure.

Materials and Methods

Animal Experiment Procedures

All animals were treated in accordance with the ARVO Statement for the Use of Animals in Ophthalmic and Vision Research and in compliance with the NIH Guide for the Care and Use of Laboratory Animals. Adult male Sprague Dawley rats were purchased from Jackson Laboratories (Bar Harbor, Maine). Animals were housed with exposure to a 12-hour light/dark cycle, constant temperature and humidity and *ad libitum* access to food and water for the duration of the study.

Hyperglycemia was induced via a single intraperitoneal (IP) injection of streptozotocin (STZ) at 65 mg/kg in sodium citrate buffer (0.01 M, pH 4.5). The diabetic state of each animal was measured using nonfasting blood glucose obtained from a tail vein nick 5 days post STZ injection. Blood glucose levels above 300 mg/dL were considered to be diabetic. Rats that did not develop hyperglycemia were excluded from the study. Body weights and nonfasting blood glucose measurements were recorded weekly throughout the study.

(−)-Nicotine hydrogen tartrate salt (Sigma, St. Louis, MO, USA) was dissolved in phosphate buffered saline and administered daily via subcutaneous injection. Nicotine treatment was initiated at 0.3 mg/kg then systematically increased until a final dose of 2.1 mg/kg was reached and was continued at this concentration for the duration of the experiment. This treatment regimen was developed experimentally to avoid acute toxicity in nicotine-naïve animals. A total of 45 rats were used in this study and were divided into 4 experimental groups: control (n=12), nicotine (n=11), diabetic (n=10) and diabetic with nicotine treatment (n=12).

Multimodal *in vivo* imaging

All animals were examined with the Spectralis™ HRA+OCT (Heidelberg Engineering, Heidelberg, Germany) to acquire baseline SD-OCT scans, fundus reflectance images, and fluorescein angiography. For subsequent imaging time points, the imaging procedure was repeated using the AutoRescan™ feature to accurately rescan the same area from the baseline imaging session. Rats were anesthetized by inhalation of isofluorane (1-3 %), pupils were dilated with 1 % tropicamide (Bausch and Lomb Inc.), and a 0.5 % Hypromellose solution (Alcon Laboratories Inc., Fort Worth, TX, USA) was applied to the cornea at regular intervals to prevent dehydration. A 20° × 20° volume scan, centered at the optic disc, was used to determine total retinal thickness (TRT) values. All SD-OCT scan were acquired in the high-resolution mode consisting of 1024 A-Scans per B-Scan. Each volume scan comprised 19 individual B-scans with an average of 20 frames per B-scan to improve the signal to noise ratio (Figure [1]). A 12° circular scan (average of 16 frames per scan) centered on the optic disc was also obtained to determine representative thickness values for individual retinal layers using segmentation software. All SD-OCT images exceeded a minimum quality threshold of 25 dB.

Following SD-OCT imaging, fluorescein angiography (FA) was performed to assess potential changes in retinal vasculature. One hundred microliters of a 1% sodium fluorescein solution (Akorn Inc., Lake Forest, IL) was administered via IP injection. Video sequences

were obtained over a 30° × 30° field of view to investigate signs of vascular leakage or changes in vessel tortuosity.

Retinal Thickness Measurements

Two independent methods were used to measure total retinal thickness (TRT) that was measured from the inner limiting membrane (ILM) to Bruch's membrane (BM). The embedded Heidelberg Eye Explorer software (Version 5.1) was used to measure TRT for the volumetric scans and assess any changes in retinal ultrastructure over the course of the study. For regional analysis, the rat retina was divided into superior, inferior, nasal and temporal quadrants using the Early Treatment Diabetic Retinopathy Study (ETDRS) grid to assess any potential variability based on retinal location within our experimental model. Retinal segmentation and TRT measurements were also performed using the OCT_Seg Program (Version 0.2) which is a freely available, MATLAB-based program originally developed by Markus Mayer (http://www5.cs.fau.de/research/software/octseg/)(45). The raw data files originally acquired with the Spectralis™ were imported into OCT_Seg and used for analysis. For our study, the rodent retina was segmented into the following layers: (1) Inner limiting membrane (ILM), ganglion cell layer (GCL), and the inner plexiform layer (IPL) (2) Inner nuclear layer (INL) and the outer plexiform layer (IPL) (3) Outer nuclear layer (ONL) (4) Photoreceptors (PR) and the retinal pigmented epithelium (RPE) as shown in Figure [2]. The segmented layers were also used to calculate TRT values. Both approaches were semi-automated and a masked grader (AB) manually corrected the delineation at the RPE/BM interface or segmented layer boundaries when necessary.

Confocal Microscopy of Retinal Flatmounts

Confocal microscopy (Zeiss LSM510META, Carl Zeiss Microscopy GmbH, Jena, Germany) was performed on retinal flatmount preparations of 3 representative animals from each treatment group to investigate changes in the retinal neurons of the GCL. Retinal flatmounts were labeled with the neuronal cell marker NeuN and vasculature with isolectin B4 with the following procedure. Enucleated eyes were fixed overnight in a 4 % solution of paraformaldehyde then the retina was carefully dissected from the eyecup. Excised tissue was blocked and permeabilized with PBS containing 1 % Triton X-100 and 10 % normal goat serum (NGS) for 30 minutes, then incubated with Alexa Fluor-594 labeled isolectin B4 and mouse NeuN antibody (MAB377, Millipore) overnight at 4° C. Next, the flatmounts were washed with PBS and incubated with Alexa Fluor 488-labeled secondary antibody (1:400; Inivitrogen, Carlsbad, CA) at room temperature for 1 hour. Finally, retinas were flat mounted in mounting medium (Vectashield; Vector Laboratories, Burlingame, CA) and examined by confocal microscopy. A 40x magnification objective was used to acquire images over a 225 μm × 225 μm area. Twelve fields were imaged for each sample along the super, inferior, nasal and temporal axes. The isolectin B4 staining of the inner retinal vessels enabled us to locate the appropriate depth of focus for the GCL. Labeled GCL neurons, including ganglion cells and amacrine cells, were then manually counted for each field of view. The mean value for each group was used to compare the differential effects of nicotine and diabetes versus the control group.

Statistical Analysis

The data for the retinal thickness measurements and GCL neuron counts exhibited normal distribution and are presented as mean ± SEM. Comparisons between treatment groups were performed using ANOVA with $P < 0.05$ considered statistically significant. Paired, 2-tailed t-tests were used to examine the longitudinal influence between the retinal thickness measurements at baseline and 8 weeks. $P < 0.05$ was considered significant.

Results

Average body weight and glucose measurements for all four groups at multiple stages of the experiment are presented in Table 1. A significant divergence in body weight was observed as the control group and nicotine exposed group continued to gain weight throughout the study. Conversely, the weights of the diabetic and nicotine exposed diabetic groups plateaued once hyperglycemia (glucose >300 mg/dl) was established. Although the body weights of the diabetic rats exposed to nicotine were generally lower, the difference was not statistically significant compared to the diabetic rats without nicotine.

Regional Retinal Thickness Values

Regional thickness values for the superior, inferior, nasal and temporal quadrants were determined based on 20° × 20° volumetric SD-OCT scans centered on the optic disc. The control group did not experience any notable changes over the course of our study while the nicotine group demonstrated significant thinning of the retina. The mean total retinal thickness (TRT) of the entire 20° × 20° volume scan for the nicotine treated group decreased by 8.3 μm following 8 weeks of systemic nicotine exposure. The inferior (−8.7 μm), nasal (−9.7 μm) and temporal (−8.4 μm) quadrants were all significantly thinner; however, thinning within the superior region (−6.4 μm) did not attain statistical significance. The diabetic group exhibited a trend for minimal retinal thinning across the entire retina, although the data did not achieve statistical significance. These findings are consistent with previously reported studies of minimal diabetic retinopathy in experimental models(11, 13, 46). The mean TRT for the diabetic group exposed to nicotine increased by 6.1 μm over the course of 8 weeks. The superior (+7.7 μm), nasal (+6.4 μm) and temporal (+5.1 μm) quadrants were significantly thicker; however, thickening of the inferior (+5.1 μm) region did not attain statistical significance. A summary of these values may be found in Table 2.

Segmented Retinal Thickness—The control group did not exhibit any changes in retinal thickness over the course of the 8 week study based on the analysis of the segmented retinal layers. The nicotine group demonstrated significant ($P < 0.05$) thinning of the ONL representing an 8 % reduction from baseline measurements while the remaining segmented layers remained unchanged. The thickness of the ONL in the diabetic group experienced a significant ($P < 0.05$) decrease of 14.4 % however; there was a trend ($P = 0.054$) toward increasing thickness in the RPE/PR region. These changes effectively offset each other yielding no significant changes in TRT. The combined effects of nicotine and diabetes resulted in a significant increase of 31 % in the segmented RPE/PR layer and a trend toward thinning in the ONL (Figure [3]). The remaining inner retinal layers for all groups did not display any changes over the course of our study.

The sum of the segmented retinal thickness values was also used to calculate the TRT for each animal at the specified imaging time points. A comparison of the TRT values measured using the Heidelberg Eye Explorer software and OCT_Seg did not reveal any statistically significant difference between the measurement techniques. In both cases, we observed a significant decrease in TRT of the nicotine group and a significant increase in the TRT of the diabetic group exposed to nicotine (Figure [4]).

Ganglion Cell Counts—Confocal microscopy was used to investigate changes in GCL neurons in all four of our experimental groups at the conclusion of the study. There was a 9.2 % decrease in the number of GCL neurons in the combined nicotine and diabetes group compared to the control group (Figure [5]) although these results did not attain statistical significance when performing ANOVA among all treatment conditions. The remaining groups did not demonstrate any notable changes in the number of GCL neurons.

Fluorescein Angiography—In addition to fundus reflectance imaging and SD-OCT, we performed fluorescein angiography (FA) to assess potential changes in vascular permeability associated with a breakdown of the blood-retina-barrier. No significant changes in vascular permeability or vessel tortuosity were observed over the course of our study *(data not shown)*.

Discussion

In the present study, we investigated the influence of nicotine in an experimentally induced diabetic rat model. Using non-invasive high resolution SD-OCT imaging, we provide for the first time, quantitative information on the temporal alterations of retinal structures at the micrometer resolution level. The reproducibility of this technique and strong correlations with histological data has already been successfully demonstrated in multiple small animal models(41, 43, 47). The ability to reliably conduct longitudinal studies on individual subjects to assess disease progression has the potential to greatly enhance our understanding of dynamic disease processes within the retina.

Cigarette smoking has been associated with progression of diabetic retinopathy(33); however complex statistical measures were warranted due to the multi-factor variability. For our study, we focused on nicotine since it is a prominent toxic ingredient in cigarettes, smokeless tobacco, electronic cigarettes, and smoking cessation products. Although our model does not encompass the breadth of toxic components found in cigarette smoke, nicotine alone has been shown to promote pathological effects on the retinal pigment epithelium, photoreceptors and cells in the outer nuclear layer in mice (37). Chronic nicotine toxicity has also been shown to increase the severity of induced choroidal neovascularization(36), diabetic nephropathy(48) and cataract development(49) in multiple experimental rodent models.

Multiple groups have reported changes in TRT as a function of DR progression using clinical SD-OCT systems(50-52); however, large patient groups were necessary to attain statistical significance. A recent report by Ciresi *et al.* questioned the clinical utility of TRT measurements to identify early DR due to the wide variability of thickness values based on

retinal location and inter-patient differences(53). As our data suggests, monitoring changes in TRT alone may not provide enough information to determine significant changes due to minimal diabetic retinopathy. However, segmentation algorithms may be applied to individual SD-OCT B-scans or volumetric data sets to determine changes in the thickness of distinct cellular layers within the retina over time.

One important finding from our study is that nicotine alone can cause deleterious effects on the rat retina as early as 8 weeks as evidenced by gradual thinning across all four quadrants studied. Upon closer inspection, the major loss of TRT may be largely attributed to the thinning of the outer nuclear layer measured using SD-OCT segmentation analysis. Interestingly, thinning in the outer nuclear layer due to nicotine toxicity in the mouse retina was recently reported by Yang *et al.* using electron microscopy following 6 months of systemic exposure(37). We were able to successfully demonstrate similar findings using *in vivo* imaging after a much shorter period of exposure, suggesting early effects of nicotine.

Additionally, we measured an increase in TRT within our combined diabetes and nicotine group. Macular edema is one of the clinical indications of DR and is observed as an increase in retinal thickness as a consequence of fluid retention in intracellular and extracellular compartments. This finding may indicate a synergistic relationship between hyperglycemia and nicotine within our experimental model leading to increased fluid retention within the retina. One explanation could be that smoking causes a reduction in blood flow due to the vasoconstrictive effects of nicotine and hypoxia due to diabetes may perturb auto-regulation leading to edema(54).

There are numerous reports of functional deficits occurring in early stage diabetic retinopathy that have been documented clinically(2, 6, 55, 56) and in animal models(10, 20) Although vascular complications are typically seen as a hallmark of the disease, the functional deficits often precede the breakdown of the blood-retina barrier, suggesting an early neurodegenerative component. Similarly, there have also been reports of functional alterations in the retina attributed to smoking(39, 40) and nicotine exposure(38). Neuronal apoptosis has been well documented in experimentally induced diabetic rodent models and in the human retina. Barber *et al*. assessed the impact of STZ-induced diabetes after 7.5 months on the neuronal retina. They found that total number of cell bodies in the retinal ganglion cell layer was reduced by 10 % accompanied by a 22 % reduction in the thickness of the inner plexiform layer and a 14 % loss in the thickness of the inner nuclear layer(5). We noted a 9.2 % decrease in the in the number of labeled GCs when comparing the combined nicotine and diabetes group to the control group based on our confocal microscopy sampling of the retinal flatmount preparations. However, this did not yield an appreciable change in the thickness of the GCL based on the *in vivo* data analysis. We were also able to demonstrate a 14.4 % thinning in the outer nuclear layer after 8 weeks of diabetes induction. One explanation in this discrepancy may be due to the differences in the methods used and the duration of each study. A significant decrease in the outer nuclear layer in a diabetic rat model using histological sections along with substantial loss in the photoreceptor layer was noted by Park *et al*. 24 weeks after the induction of diabetes(11). Collectively, these studies suggest that neural retinal changes may be an early pathological indicator prior to microvasculopathy. The development of cataracts was a limiting factor in

the temporal evaluation of our non-invasive imaging study. Despite the duration of our study, we were still able to demonstrate significant changes in retinal morphology attributed to nicotine, diabetes and potential synergistic effects accelerating degeneration of neuronal cells. Future studies investigating additional animal models and clinical data may provide additional insight into the mechanisms responsible.

It is also important to note that we used one retinal segmentation approach but there are numerous algorithms and software packages available to perform such analysis. Moreover, new techniques and applications are continually being developed and refined to investigate a wide variety of conditions. Although it is beyond scope of our paper to discuss these techniques, a recent review by Abramoff *et al*.(57) is an excellent resource for further information.

In conclusion, we observed detrimental changes in the rat retina due to systemic nicotine exposure and in combination with experimentally induced diabetes using non-invasive SD-OCT imaging and morphologic analysis of GCL neurons. Our quantitative analysis demonstrated the neurodegenerative influence of nicotine, experimental diabetes, and their combined effects on the retinal ultrastructure. Utilizing new analytical techniques with existing clinical diagnostics may provide additional insights into the dynamics of progressive retinal diseases such as DR. A better understanding of the influence of environmental risk factors may help in life style change, thereby limiting the complications associated with DR.

Acknowledgments

Funding

Support: National Institute of Environmental Health Sciences; Research to Prevent Blindness (RPB), "This study was conducted with the support of the Institute for Translational Sciences at the University of Texas Medical Branch, supported in part by a Clinical and Translational Science Award (UL1TR000071) from the National Center for Advancing Translational Sciences, National Institutes of Health." (MM); NIH Grant EY022694, American Heart Association 11SDG4960005, and International Retinal Research Foundation (W.Z.).

References

1. Zheng Y, He M, Congdon N. The worldwide epidemic of diabetic retinopathy. Indian J Ophthalmol. 2012; 60(5):428–31. [PubMed: 22944754]
2. Jackson GR, Barber AJ. Visual dysfunction associated with diabetic retinopathy. Curr Diab Rep. 2010; 10(5):380–4. [PubMed: 20632133]
3. Tarr JM, Kaul K, Wolanska K, Kohner EM, Chibber R. Retinopathy in diabetes. Adv Exp Med Biol. 2012; 771:88–106. [PubMed: 23393674]
4. Holopigian K, Greenstein VC, Seiple W, Hood DC, Carr RE. Evidence for photoreceptor changes in patients with diabetic retinopathy. Invest Ophthalmol Vis Sci. 1997; 38(11):2355–65. [PubMed: 9344359]
5. Barber AJ, Lieth E, Khin SA, Antonetti DA, Buchanan AG, Gardner TW. Neural apoptosis in the retina during experimental and human diabetes. Early onset and effect of insulin. J Clin Invest. 1998; 102(4):783–91. [PubMed: 9710447]
6. Lieth E, Gardner TW, Barber AJ, Antonetti DA, Group PSRR. Retinal neurodegeneration: early pathology in diabetes. Clin Experiment Ophthalmol. 2000; 28(1):3–8. [PubMed: 11345341]
7. Zeng XX, Ng YK, Ling EA. Neuronal and microglial response in the retina of streptozotocin-induced diabetic rats. Vis Neurosci. 2000; 17(3):463–71. [PubMed: 10910112]

8. Lorenzi M, Gerhardinger C. Early cellular and molecular changes induced by diabetes in the retina. Diabetologia. 2001; 44(7):791–804. [PubMed: 11508263]
9. Gardner TW, Antonetti DA, Barber AJ, LaNoue KF, Levison SW. Diabetic retinopathy: more than meets the eye. Surv Ophthalmol. 2002; 47(Suppl 2):S253–62. [PubMed: 12507627]
10. Li Q, Zemel E, Miller B, Perlman I. Early retinal damage in experimental diabetes: electroretinographical and morphological observations. Exp Eye Res. 2002; 74(5):615–25. [PubMed: 12076083]
11. Park SH, Park JW, Park SJ, Kim KY, Chung JW, Chun MH, et al. Apoptotic death of photoreceptors in the streptozotocin-induced diabetic rat retina. Diabetologia. 2003; 46(9):1260–8. [PubMed: 12898017]
12. Barber AJ. A new view of diabetic retinopathy: a neurodegenerative disease of the eye. Prog Neuropsychopharmacol Biol Psychiatry. 2003; 27(2):283–90. [PubMed: 12657367]
13. Martin PM, Roon P, Van Ells TK, Ganapathy V, Smith SB. Death of retinal neurons in streptozotocin-induced diabetic mice. Invest Ophthalmol Vis Sci. 2004; 45(9):3330–6. [PubMed: 15326158]
14. van Dijk HW, Kok PH, Garvin M, Sonka M, Devries JH, Michels RP, et al. Selective loss of inner retinal layer thickness in type 1 diabetic patients with minimal diabetic retinopathy. Invest Ophthalmol Vis Sci. 2009; 50(7):3404–9. [PubMed: 19151397]
15. van Dijk HW, Verbraak FD, Kok PH, Garvin MK, Sonka M, Lee K, et al. Decreased retinal ganglion cell layer thickness in patients with type 1 diabetes. Invest Ophthalmol Vis Sci. 2010; 51(7):3660–5. [PubMed: 20130282]
16. Bronson-Castain KW, Bearse MA, Neuville J, Jonasdottir S, King-Hooper B, Barez S, et al. Early Neural And Vascular Changes In The Adolescent Type 1 And Type 2 Diabetic Retina. Retina. 2011
17. Ghirlanda G, Di Leo MA, Caputo S, Falsini B, Porciatti V, Marietti G, et al. Detection of inner retina dysfunction by steady-state focal electroretinogram pattern and flicker in early IDDM. Diabetes. 1991; 40(9):1122–7. [PubMed: 1936619]
18. Di Leo MA, Falsini B, Caputo S, Ghirlanda G, Porciatti V, Greco AV. Spatial frequency-selective losses with pattern electroretinogram in type 1 (insulin-dependent) diabetic patients without retinopathy. Diabetologia. 1990; 33(12):726–30. [PubMed: 2073985]
19. Sima AA, Zhang WX, Cherian PV, Chakrabarti S. Impaired visual evoked potential and primary axonopathy of the optic nerve in the diabetic BB/W-rat. Diabetologia. 1992; 35(7):602–7. [PubMed: 1644237]
20. Aung MH, Kim MK, Olson DE, Thule PM, Pardue MT. Early visual deficits in streptozotocin-induced diabetic long evans rats. Invest Ophthalmol Vis Sci. 2013; 54(2):1370–7. [PubMed: 23372054]
21. Solberg Y, Rosner M, Belkin M. The association between cigarette smoking and ocular diseases. Surv Ophthalmol. 1998; 42(6):535–47. [PubMed: 9635902]
22. Thornton J, Edwards R, Mitchell P, Harrison RA, Buchan I, Kelly SP. Smoking and age-related macular degeneration: a review of association. Eye (Lond). 2005; 19(9):935–44. [PubMed: 16151432]
23. Neuner B, Komm A, Wellmann J, Dietzel M, Pauleikhoff D, Walter J, et al. Smoking history and the incidence of age-related macular degeneration--results from the Muenster Aging and Retina Study (MARS) cohort and systematic review and meta-analysis of observational longitudinal studies. Addict Behav. 2009; 34(11):938–47. [PubMed: 19539431]
24. Cano M, Thimmalappula R, Fujihara M, Nagai N, Sporn M, Wang AL, et al. Cigarette smoking, oxidative stress, the anti-oxidant response through Nrf2 signaling, and Age-related Macular Degeneration. Vision Res. 2010; 50(7):652–64. [PubMed: 19703486]
25. Edwards R, Thornton J, Ajit R, Harrison RA, Kelly SP. Cigarette smoking and primary open angle glaucoma: a systematic review. J Glaucoma. 2008; 17(7):558–66. [PubMed: 18854733]
26. Zhang X, Kahende J, Fan AZ, Barker L, Thompson TJ, Mokdad AH, et al. Smoking and visual impairment among older adults with age-related eye diseases. Prev Chronic Dis. 2011; 8(4):A84. [PubMed: 21672408]

27. Kelly SP, Thornton J, Edwards R, Sahu A, Harrison R. Smoking and cataract: review of causal association. J Cataract Refract Surg. 2005; 31(12):2395–404. [PubMed: 16473237]
28. Galor A, Lee DJ. Effects of smoking on ocular health. Curr Opin Ophthalmol. 2011; 22(6):477–82. [PubMed: 21897240]
29. Eliasson B. Cigarette smoking and diabetes. Prog Cardiovasc Dis. 2003; 45(5):405–13. [PubMed: 12704597]
30. Lois N, Abdelkader E, Reglitz K, Garden C, Ayres JG. Environmental tobacco smoke exposure and eye disease. Br J Ophthalmol. 2008; 92(10):1304–10. [PubMed: 18658170]
31. Will JC, Galuska DA, Ford ES, Mokdad A, Calle EE. Cigarette smoking and diabetes mellitus: evidence of a positive association from a large prospective cohort study. Int J Epidemiol. 2001; 30(3):540–6. [PubMed: 11416080]
32. Karamanos B, Porta M, Songini M, Metelko Z, Kerenyi Z, Tamas G, et al. Different risk factors of microangiopathy in patients with type I diabetes mellitus of short versus long duration. The EURODIAB IDDM Complications Study. Diabetologia. 2000; 43(3):348–55. [PubMed: 10768096]
33. Mühlhauser I, Bender R, Bott U, Jörgens V, Grüsser M, Wagener W, et al. Cigarette smoking and progression of retinopathy and nephropathy in type 1 diabetes. Diabet Med. 1996; 13(6):536–43. [PubMed: 8799657]
34. Chase HP, Garg SK, Marshall G, Berg CL, Harris S, Jackson WE, et al. Cigarette smoking increases the risk of albuminuria among subjects with type I diabetes. JAMA. 1991; 265(5):614–7. [PubMed: 1987411]
35. Heeschen C, Jang JJ, Weis M, Pathak A, Kaji S, Hu RS, et al. Nicotine stimulates angiogenesis and promotes tumor growth and atherosclerosis. Nat Med. 2001; 7(7):833–9. [PubMed: 11433349]
36. Suñer IJ, Espinosa-Heidmann DG, Marin-Castano ME, Hernandez EP, Pereira-Simon S, Cousins SW. Nicotine increases size and severity of experimental choroidal neovascularization. Invest Ophthalmol Vis Sci. 2004; 45(1):311–7. [PubMed: 14691189]
37. Yang L, Gong H, Wang Y, Yin H, Chen P, Zhang H. Nicotine alters morphology and function of retinal pigment epithelial cells in mice. Toxicol Pathol. 2010; 38(4):560–7. [PubMed: 20448088]
38. Varghese SB, Reid JC, Hartmann EE, Keyser KT. The effects of nicotine on the human electroretinogram. Invest Ophthalmol Vis Sci. 2011; 52(13):9445–51. [PubMed: 22064991]
39. Gundogan FC, Durukan AH, Mumcuoglu T, Sobaci G, Bayraktar MZ. Acute effects of cigarette smoking on pattern electroretinogram. Doc Ophthalmol. 2006; 113(2):115–21. [PubMed: 16972083]
40. Gundogan FC, Erdurman C, Durukan AH, Sobaci G, Bayraktar MZ. Acute effects of cigarette smoking on multifocal electroretinogram. Clin Experiment Ophthalmol. 2007; 35(1):32–7. [PubMed: 17300568]
41. Huber G, Beck SC, Grimm C, Sahaboglu-Tekgoz A, Paquet-Durand F, Wenzel A, et al. Spectral domain optical coherence tomography in mouse models of retinal degeneration. Invest Ophthalmol Vis Sci. 2009; 50(12):5888–95. [PubMed: 19661229]
42. Zhou Y, Sheets KG, Knott EJ, Regan CE, Tuo J, Chan CC, et al. Cellular and 3D optical coherence tomography assessment during the initiation and progression of retinal degeneration in the Ccl2/Cx3cr1-deficient mouse. Exp Eye Res. 2011; 93(5):636–48. [PubMed: 21854772]
43. Fischer MD, Huber G, Beck SC, Tanimoto N, Muehlfriedel R, Fahl E, et al. Noninvasive, in vivo assessment of mouse retinal structure using optical coherence tomography. PLoS One. 2009; 4(10):e7507. [PubMed: 19838301]
44. Knott EJ, Sheets KG, Zhou Y, Gordon WC, Bazan NG. Spatial correlation of mouse photoreceptor-RPE thickness between SD-OCT and histology. Exp Eye Res. 2011; 92(2):155–60. [PubMed: 21035444]
45. Mayer MA, Hornegger J, Mardin CY, Tornow RP. Retinal Nerve Fiber Layer Segmentation on FD-OCT Scans of Normal Subjects and Glaucoma Patients. Biomed Opt Express. 2010; 1(5):1358–83. [PubMed: 21258556]
46. Luan H, Roberts R, Sniegowski M, Goebel DJ, Berkowitz BA. Retinal thickness and subnormal retinal oxygenation response in experimental diabetic retinopathy. Invest Ophthalmol Vis Sci. 2006; 47(1):320–8. [PubMed: 16384980]

47. Gabriele ML, Ishikawa H, Schuman JS, Bilonick RA, Kim J, Kagemann L, et al. Reproducibility of spectral-domain optical coherence tomography total retinal thickness measurements in mice. Invest Ophthalmol Vis Sci. 2010; 51(12):6519–23. [PubMed: 20574022]

48. Hua P, Feng W, Ji S, Raij L, Jaimes EA. Nicotine worsens the severity of nephropathy in diabetic mice: implications for the progression of kidney disease in smokers. Am J Physiol Renal Physiol. 2010; 299(4):F732–9. [PubMed: 20685820]

49. Tirgan N, Kulp GA, Gupta P, Boretsky A, Wiraszka TA, Godley B, et al. Nicotine Exposure Exacerbates Development of Cataracts in a Type 1 Diabetic Rat Model. Experimental Diabetes Research. 2012; 2012:7.

50. Biallosterski C, van Velthoven ME, Michels RP, Schlingemann RO, DeVries JH, Verbraak FD. Decreased optical coherence tomography-measured pericentral retinal thickness in patients with diabetes mellitus type 1 with minimal diabetic retinopathy. Br J Ophthalmol. 2007; 91(9):1135–8. [PubMed: 17383994]

51. Cho HY, Lee DH, Chung SE, Kang SW. Diabetic retinopathy and peripapillary retinal thickness. Korean J Ophthalmol. 2010; 24(1):16–22. [PubMed: 20157409]

52. Lattanzio R, Brancato R, Pierro L, Bandello F, Iaccher B, Fiore T, et al. Macular thickness measured by optical coherence tomography (OCT) in diabetic patients. Eur J Ophthalmol. 2002; 12(6):482–7. [PubMed: 12510717]

53. Ciresi A, Amato MC, Morreale D, Morreale R, Di Giovanna F, Carità S, et al. OCT is not useful for detection of minimal diabetic retinopathy in type 1 diabetes. Acta Diabetol. 2010; 47(3):259–63. [PubMed: 20454812]

54. Morgado PB, Chen HC, Patel V, Herbert L, Kohner EM. The acute effect of smoking on retinal blood flow in subjects with and without diabetes. Ophthalmology. 1994; 101(7):1220–6. [PubMed: 8035985]

55. Bearse MA, Han Y, Schneck ME, Barez S, Jacobsen C, Adams AJ. Local multifocal oscillatory potential abnormalities in diabetes and early diabetic retinopathy. Invest Ophthalmol Vis Sci. 2004; 45(9):3259–65. [PubMed: 15326149]

56. Han Y, Adams AJ, Bearse MA, Schneck ME. Multifocal electroretinogram and short-wavelength automated perimetry measures in diabetic eyes with little or no retinopathy. Arch Ophthalmol. 2004; 122(12):1809–15. [PubMed: 15596584]

57. Abràmoff MD, Garvin MK, Sonka M. Retinal imaging and image analysis. IEEE Rev Biomed Eng. 2010; 3:169–208. [PubMed: 22275207]

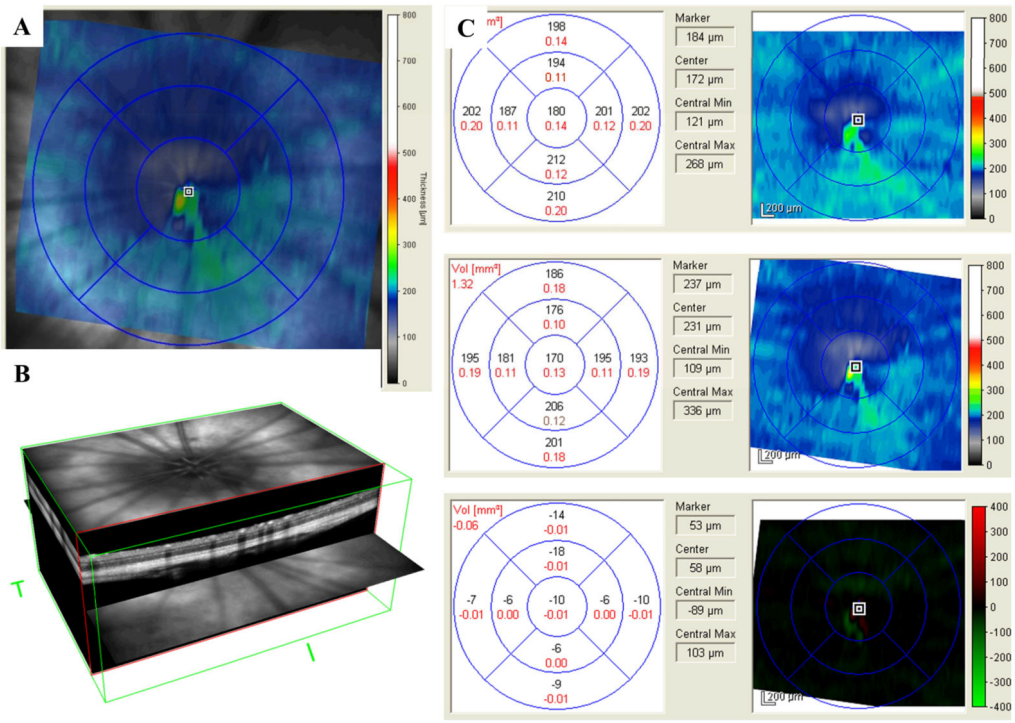

Figure 1.

Morphometric analysis of the rat retina non-invasively using SD-OCT. (A) SLO fundus image with corresponding overlay of the 20° × 20° field of view used for volumetric SD-OCT in the rat retina. (B) 3-D reconstruction of the retinal volume used to perform regional TRT measurements. (C) Example of the regional TRT thickness measurements performed for each animal utilizing the TruTrack™ registration method and Heidelberg Engineering Eye Explorer version 5.1 analytical software (Baseline, 8 week follow up, differential retinal thickness map).

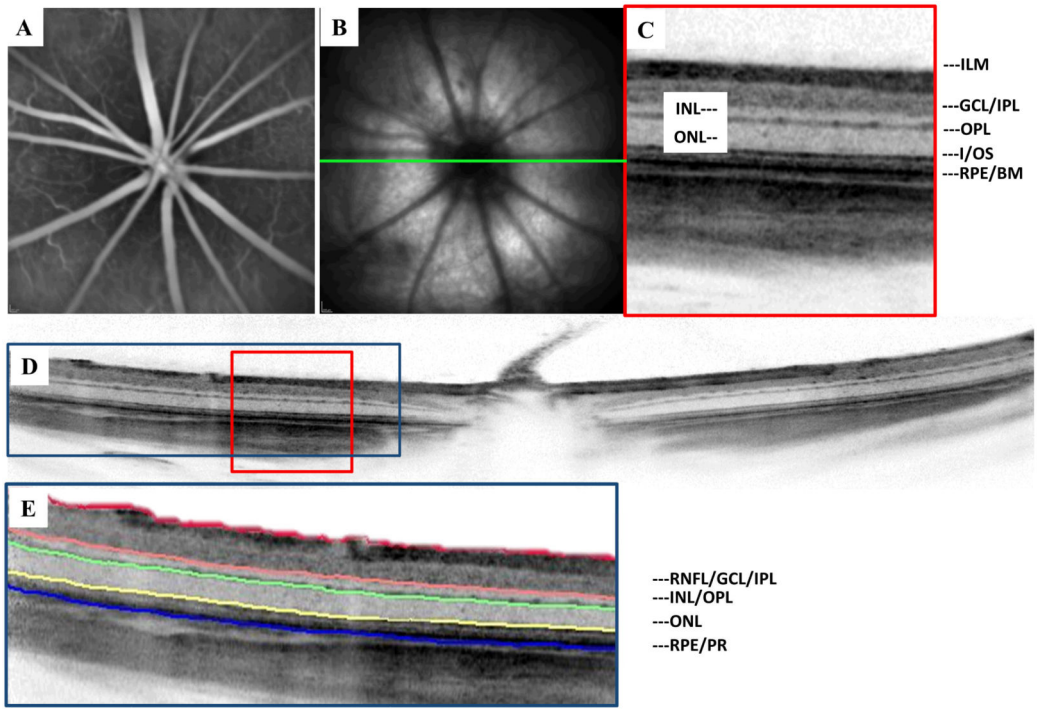

Figure 2.

Multimodal imaging of the Sprague Dawley rat retina. (A) Fluorescein angiography highlighting the retinal vasculature (B) NIR reflectance SLO of the albino rat fundus. (C) Observed retinal layers using high resolution SD-OCT (D) Single 20° B-scan centered on the optic disc representing an average of 20 frames (E) Depiction of the retinal layers segmented and measured using OCT_Seg.

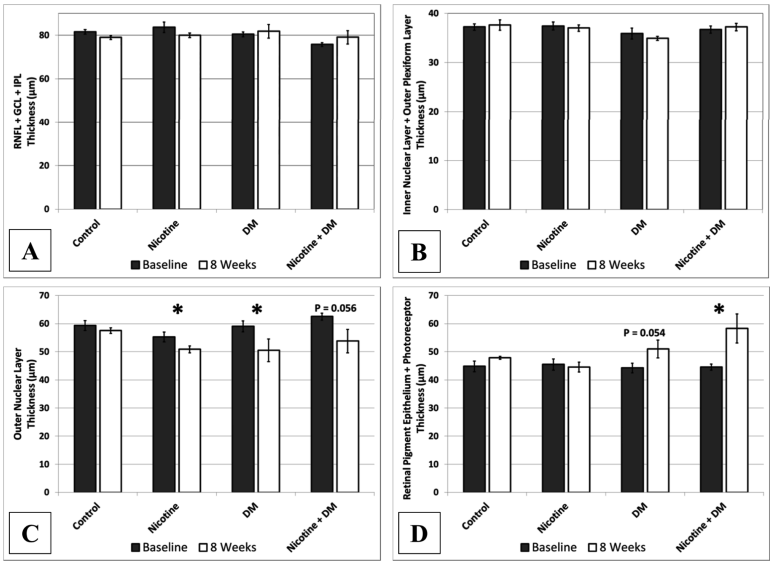

Figure 3.

Segmented retinal thickness values were divided into 4 groups based on our ability to effectively delineate layer boundaries using the semi-automated technique. (A) The innermost layers of the RNFL, GCL and IPL did not demonstrate any significant changes in SD-OCT morphology associated with nicotine exposure or diabetes. (B) Likewise, the INL and OPL remained unchanged for all groups after 8 weeks. (C) The ONL was significantly thinner in the nicotine group and the diabetic group. (D)The outer retina measured from the RPE/BM interface to the IS/OS junction demonstrated a significant increase in thickness associated with the combination of nicotine exposure and diabetes.

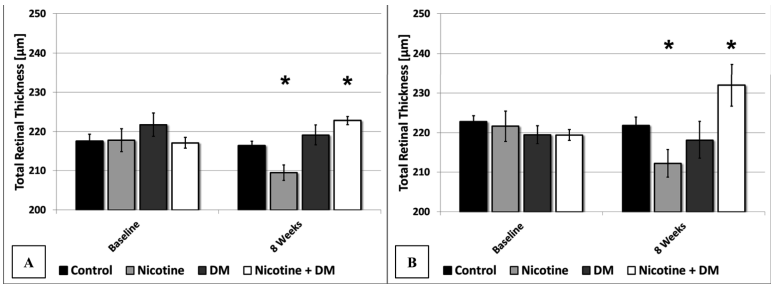

Figure 4.

Independent methods of analyzing TRT values yielded similar results in terms of significance with respect to retinal thinning in the nicotine exposed animals and retinal thickening in the DM group exposed to nicotine. Embedded Heidelberg Eye Explorer software (A) and OCT_Seg (B) yielded significant differences in both the nicotine exposed group and the combined nicotine and diabetes group after eight weeks. On average, the segmentation software measurements of TRT were 5.5 μm greater than the Heidelberg Eye Explorer software. For both measurement techniques, ANOVA among treatment groups at 8 weeks ($P < 0.001$). *Two-tailed t-test demonstrating statistically significant difference from baseline ($P < 0.05$)

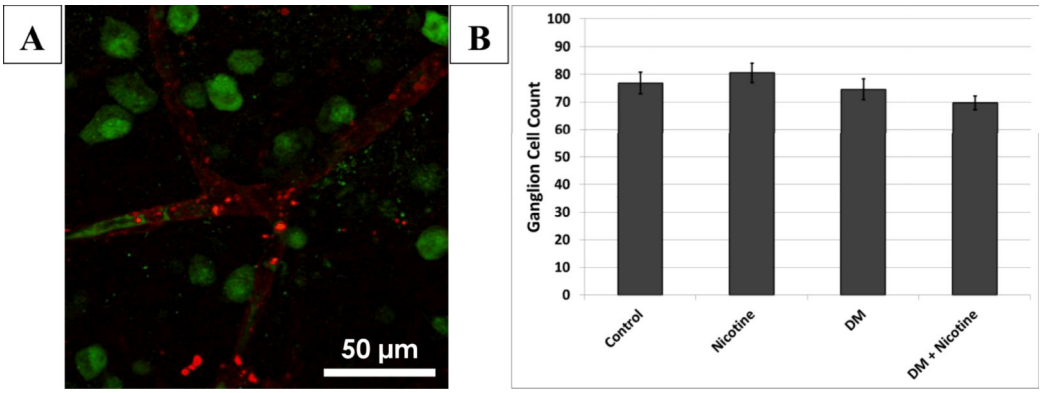

Figure [5].

Confocal microscopy of labeled neurons in the ganglion cell layer (GCL) from flatmount preparations. Mean neuronal cell density was determined based on 12 confocal imaging fields (40X) in 3 representative animals from each treatment group. GCL was identified by the proximity to inner retinal vasculature. The data represent mean ± SEM for each image based on the experimental group (A) maximum intensity projection of an enhanced field of view is shown. (B) A 9.2% reduction in the density of stained GCL neurons was noted between the control group and the diabetic group treated with nicotine although no significant differences were observed at the conclusion of our study based on ANOVA ($P > 0.05$), Red: isolectin B4 staining of the vasculature, Green: GCL Neurons. Scale bar = 50 µm.

Table 1

Average Body Weights and Blood Glucose Levels for Each Treatment Group

Duration of Diabetes (Weeks)	Treatment Group	*n*	Weight (g)	Blood Glucose (mg/dL)
2	Control	12	485.8 ± 21.8	119.7 ± 6.5
	Nicotine	12	493.0 ± 20.0	123.2 ± 8.8
	Diabetic	10	365.2 ± 12.0*†	638.2 ± 23.5*†
	Diabetic + Nicotine	11	337.1 ± 18.4*†	581.9 ± 29.4*†
4	Control	12	517.3 ± 17.9	115.4 ± 4.8
	Nicotine	12	515.5 ± 16.9	128.5 ± 8.9
	Diabetic	10	360.5 ± 11.2*†	545.5 ± 36.7*†
	Diabetic + Nicotine	11	327.8 ± 18.3*†	573.3 ± 41.l*†
8	Control	12	565.0 ± 15.4	111.5 ± 5.4
	Nicotine	12	566.5 ± 15.2	119.2 ± 8.4
	Diabetic	10	380.5 ± 11.l*†	571.6 ± 19.9*†
	Diabetic + Nicotine	11	347.7 ± 20.7*†	552.6 ± 15.0*†

Data are expressed as mean ± SEM

*Significant difference from Control Group ($P < 0.05$)

†Significant difference from Nicotine Exposed Group ($P<0.05$)

Table 2

Regional retinal thickness values from volumetric SD-OCT scans

		Superior (μm)	Inferior (μm)	Nasal (μm)	Temporal (μm)	TRT (μm)
Control	*Baseline*	211.6± 2.3	225.4 ± 2.2	216.5 ± 1.8	216.8 ± 2.2	217.6 ± 1.8
	8 Weeks	212.1 ± 1.7	223.5 ± 2.0	213.8 ± 1.5	216.1 ± 1.6	216.4 ± 1.2
Nicotine	*Baseline*	211.8 ± 3.0	223.7 ± 3.3	219.3 ± 2.9	216.4 ± 3.1	217.8 ± 3.0
	8 Weeks	205.4 ± 2.6	**215.0 ± 1.8** *	**209.6 ± 1.8** *	**208.0 ± 2.2** *	**209.5 ± 2.0** *
DM	*Baseline*	216.2 ± 3.1	227.9 ± 3.1	221.8 ± 3.0	221.2 ± 3.0	221.9 ± 2.8
	8 Weeks	215.8 ± 3.6	223.6 ± 2.7	221.1 ± 2.5	217.4 ± 3.4	219.6 ± 2.7
Nicotine + DM	*Baseline*	213.8 ± 2.2	221.7 ± 1.4	216.9 ± 1.3	215.8 ± 1.5	217.1 ± 1.2
	8 Weeks	**221.5 ± 1.7** *	**226.6 ± 2.0**	**223.3 ± 1.2** *	**220.9 ± 1.4** *	**223.2 ± 1.0** *

Values are mean ± SEM

* $P < 0.05$, compared to baseline values